The Evolution of Al-Li Base Products for Aerospace and Space Applications

ROBERTO J. RIOJA and JOHN LIU

A technical review of the physical, mechanical, and metallurgical variables that have influenced performance of Al-Li based alloys over the last 50 years is presented. First, the historic evolution of different alloys is discussed. Then, the microstructural features responsible for different mechanical properties are identified and discussed. The role of alloying additions is discussed. The shortcomings of a 2nd generation Al-Li alloys are introduced and the key alloy design principles used to overcome these are discussed. Finally, the performance parameters that play a major role in sizing several aircraft and space craft components are reviewed in a chronological perspective and compared with 3rd-generation Al–Li alloys. It is concluded that significant improvements have been made to position Al–Li alloys to enable improved performance of next generation of air and space craft.

DOI: 10.1007/s11661-012-1155-z

I. INTRODUCTION

HISTORICALLY, improvements in the performance of aerospace and space craft have been based on improvements in the performance of metallic materials. The specific properties (property/density) of aluminum-based alloys and products* have increased over time as the aerospace industry has evolved. Starting with the Wright brothers' flight in 1903, an Al-9 wt pct Cu cast product was used in the crankcase of the engine. This alloy had specific yield strength of 43 (MPa/gm/cm^3).[1] Today's strongest aerospace aluminum plate product is 7055-T7751, which is used for upper wings. The specific compressive strength of 7055-T7751 plate product is 229 (MPa/gm/cm^3),[2] *i.e.*, more than five times stronger.

*For the purposes of this article, an alloy is a mixture of chemical elements as defined by the Aluminum Association designation. A product consists of an alloy with a temper and has a physical shape and measurable attributes.

The space tanks used to propel payload into space have undergone a similar evolution. The Saturn IB, which was present at the start of the space race, had fuel tanks made with 5456–H116 plate. The specific yield strength of 5456-H116 is 96 (MPa/gm/cm^3). In comparison, the fuel tanks of the space shuttle made with 2195-T8M4 plate show a specific yield strength of 211 (MPa/gm/cm^3).

Improvements in specific strength are not the only indicator of improved performance for aerospace materials. Durability (*e.g.*, corrosion and fatigue resistance) and damage tolerance (*e.g.*, residual strength and fatigue crack growth) properties often determine the size of the aircraft components. The properties of most importance are a function of the aircraft component (*e.g.*, upper or lower wing, fuselage, empennage, *etc.*) and position on the aircraft.[2]

The Al-Li products offer opportunities for significant improvements in aerostructural performance through density reduction, stiffness increase, increases in fracture toughness and fatigue crack growth resistance, and enhanced corrosion resistance. However, previous generations of Al-Li alloy products (*e.g.*, 2090-T81 plate, 8090-T86 plate, and 2091-T84 sheet) exhibited significant in-plane and through-thickness anisotropy in mechanical properties. These yielded undesirable design and manufacturing characteristics such as crack deviation and microcracking during cold hole expansion. In addition, they showed low short-transverse fracture toughness, poor corrosion resistance, and poor thermal stability. In this article, the results of intense research and development (R&D) are discussed to demonstrate the understanding of the underlying metallurgical causes for the undesirable characteristics. This work has culminated in key alloy design principles that have led to the successful development and commercialization of the 3rd generation Al-Li alloys with highly desirable combinations of properties. The evolution of key properties for upper wing, lower wing, fuselage, and space applications is discussed. These new Al-Li products, in combination with advanced design concepts, offer opportunities for improved structural performance for next generation aerospace applications.

II. TECHNICAL REASONS FOR ALLOYING ALUMINUM ALLOYS WITH LI ADDITIONS

- 1 wt pct Li addition provides approximately 3 pct decrease in density.

ROBERTO J. RIOJA, Alcoa Technical Fellow, and JOHN LIU, Director of Aerospace and Materials Technology, are with the Alcoa Technical Center, 100 Technical Drive, Alcoa Center, PA 15069. Contact e-mail: roberto.rioja@alcoa.com
Manuscript submitted October 28, 2011.
Article published online March 31, 2012

- 1 wt pct Li addition provides approximately 6 pct increase in Young's elastic modulus.
- Li additions enable the formation of potent hardening precipitates.
- Li additions impart higher fatigue crack growth resistance.

References 3 through 8 provide different summaries of the preceding reasons.

III. HISTORICAL DEVELOPMENT OF AL-LI ALLOYS

A. *The First Generation*

Work on Li additions to Al was reported as early as the mid 1920s, but it was not until 1945 when I. M. Le Baron of Alcoa patented the first Al-Li-Cu compositions.[9] The first aircraft application of Al-Li alloys was in the form of 2020 plate in 1958 used in the wings of the Navy's RA-5C Vigilante aircraft (see Table I).

This aircraft was retired after 20 years of service life with no reported cracks or corrosion issues. Follow-up work in the former Soviet Union led to the development of plate from alloy VAD23 (similar to 2020) and the development of plate, sheet, extrusions, and forgings from alloys 01420 and 01421, which have been used significantly in Soviet aircraft.[10]

B. *Second-Generation Al-Li Products*

Al-Li R&D in the late 1970s and early 1980s focused on a gauge-for-gauge substitution of wrought products, with the key objective of capturing weight savings by lower density. Alcoa focused on a 7075-T6 replacement with the development of a 2090-T81 plate, 2090-T86 extrusions, and 2090-T83 and T84 sheet. Pechiney (from France) focused their efforts on a substitute for a 2024-T3 sheet and light gauge products, and a 2091-T8X was developed.[11,12] The British Aerospace Establishment also developed a substitute for 2024-T3 sheet and light gauge plate (*e.g.*, 8090-T81plate) and licensed the technology to British Alcan.[5] The same alloy, in a T87 temper, was developed as a medium-strength, heavy-gauge plate product for space applications. The former Soviets developed their own versions of the European and American developments, and in the late 1980s, they disclosed the technical merits of 01430 (like 2091), 01440 (like 8090), and 01450 and 01460 (like 2090) wrought products.[10,12]

In general, the preceding "2nd generation Al-Li products" contained Li concentrations above 2 wt pct. Although density reduction was clearly attractive, these products exhibited several characteristics that were considered undesirable by airframe designers.

The key positive performance attributes for the 2nd-generation Al-Li products were as follows:

- Lower density (from 7 pct to 10 pct)
- Higher modulus of elasticity (from 10 pct to 15 pct)
- Higher fatigue life (lower fatigue crack growth rates)

The key negative performance attributes for 2nd generation Al-Li products were as follows:

- Lower short-transverse fracture toughness
- Lower plane stress (K_c) fracture toughness/residual strength in sheet
- Higher anisotropy of tensile properties

Table I. Nominal Composition of Key Al-Li Alloys

	Li	Cu	Mg	Ag	Zr	Sc	Mn	Zn	Approximate Date
1st generation									
2020	1.2	4.5					0.5		Alcoa 1958
01420	2.1		5.2		0.11				Soviet 1965
01421	2.1		5.2		0.11	0.17			Soviet 1965
2nd generation (Li ≥ 2 pct)									
2090	2.1	2.7			0.11				Alcoa 1984
2091	2.0	2.0	1.3		0.11				Pechiney 1985
8090	2.4	1.2	0.8		0.11	0.17			EAA 1984
01430	1.7	1.6	2.7		0.11				Soviet 1980s
01440	2.4	1.5	0.8		0.11				Soviet 1980s
01450	2.1	2.9			0.11				Soviet 1980s
01460	2.25	2.9			0.11	0.09			Soviet 1980s
3rd generation (Li < 2 pct)									
2195	1.0	4.0	0.4	0.4	0.11				LM/Reynolds 1992
2196	1.75	2.9	0.5	0.4	0.11		0.35 max	0.35 max	LM/Reynolds 2000
2297	1.4	2.8	0.25 max		0.11		0.3	0.5 max	LM/Reynolds 1997
2397	1.4	2.8	0.25 max		0.11		0.3	0.10	Alcoa 1993
2198	1.0	3.2	0.5	0.4	0.11		0.5 max	0.35 max	Reynolds/McCook 2005
2099	1.8	2.7	0.3		0.09		0.3	0.7	Alcoa 2003
2199	1.6	2.6	0.2		0.09		0.3	0.6	Alcoa 2005
2050	1.0	3.6	0.4	0.4	0.11		0.35	0.25 max	Pechiney 2004
2060	0.75	3.95	0.85	0.25	0.11		0.3	0.4	Alcoa 2011
2055	1.15	3.7	0.4	0.4	0.11		0.3	0.5	Alcoa 2012

C. *The Third Generation*

A root-cause analysis of the shortcomings of 2nd generation Al-Li alloys led to the development of new alloys with reduced Li concentration (from 0.75 to 1.8 wt pct) since the late 1980s. Alloys 2195, 2196, 2297, 2397, 2198, 2099, 2199, 2050, 2060, and C99N (Table I) were researched and developed for space and aircraft applications, and they are referred to as 3rd-generation Al-Li Products.[12]

D. *Key Alloy Design Principles Leading to the Success of 3rd-Generation Al-Li Alloys*

Understanding the influence of chemical composition and microstructure on mechanical and corrosion performance led to the simultaneous optimization of alloying additions and thermal-mechanical processing (TMP).

The following alloying additions are involved in the development of 3rd-generation alloys and products:

- Li and Mg for density reduction, and solid-solution and precipitation strengthening
- Cu and Ag for solid-solution and precipitation strengthening
- Zn for solid-solution strengthening and corrosion improvement
- Zr and Mn for control of recrystallization and texture
- Fe and Si as impurities affecting fracture toughness, fatigue, and corrosion
- Ti as a grain refiner during solidification of ingots
- Na and K as impurities affecting fracture toughness

The following precipitates are involved in strengthening: T_1 (Al_2CuLi), δ' (Al_3Li), and θ'-type (~Al_2Cu). Here, it is proposed that the addition of Mg and Ag leads to the formation of omega (Ω) precipitates that are isomorphous and isostructural with the T_1 phase. In this context, the Ag atoms substitute Cu atomic positions and the Mg atoms substitute Li atomic positions in the T_1 structure leading to Al_2 (Cu-Ag)(Li-Mg) stochiometry and atomic arrangements. The θ'-type precipitates are thought to be isomorphous and isostructural with θ' precipitates in the Al-Cu system. Once Li is added, however, it is postulated that the Li atoms could substitute into the defect sites of the CaF_2-prototype lattice.[13] References 14 and 15 provide a comprehensive summary discussion on the structures of strengthening metastable phases in Al-Li products. Reference 16 provides a comprehensive mechanism for T_1 nucleation and growth. To control the recrystallization and texture of wrought products, the dispersoids that form in most 3rd-generation products are Al_3Zr and $Al_{20}Cu_2Mn_3$.

In the presence of Cu, the Fe forms an insoluble constituent phase with the Al_7Cu_2Fe stoichiometry and crystal structure. This phase is minimized because it affects the fracture toughness and fatigue adversely.

The influence of cold deformation (stretching, cold rolling, and cold compressing) prior to aging is highly beneficial to the strength and fracture toughness of 3rd-generation Al-Li products. This is because of the refinement of precipitate microstructures and discouragement of precipitation at grain boundaries during aging.[17,18] The pronounced effect of cold deformation prior to aging on strength and toughness in Al-Li products is caused by the high propensity of the T_1 phase to nucleate on dislocations. Cold work prior to aging increases the number of T_1 precipitates by approximately two orders of magnitude.[17,18]

As an example, 2099 and 2199 products (see Table I for composition) exploit the following precipitates, dispersoids, and elements for their attractive properties:

- Strengthening: T_1 (Al_2CuLi), δ' (Al_3Li), and θ'-type (~Al_2Cu), Mg
- Toughness control: T_1 (Al_2CuLi), T_2 (Al_6CuLi_3), β' (Al_3Zr), and $Al_{20}Cu_2Mn_3$
- Recrystallization Control: Coherent β' (Al_3Zr) dispersoids
- Grain size and texture control: $Al_{20}Cu_2Mn_3$ dispersoids
- Fatigue improvement: incoherent $Al_{20}Cu_2Mn_3$ dispersoids, δ' (Al_3Li)
- Improvement in corrosion resistance: Zn

A schematic diagram of the precipitate microstructure is shown in Figure 1.

The typical strengthening precipitates in 3rd-generation Al-Li Alloys are shown in the following dark-field TEM micrographs (Figure 2).

Textures describe preferred crystallographic orientation of grains and subgrains in a given direction. They are produced or changed during deformation processes (*e.g.*, rolling and extrusion) and thermal processes (*e.g.*, recovery or recrystallization annealing). Al-Li alloy products can be controlled by TMP and alloy constitution to be either unrecrystallized or recrystallized microstructures.[12,19]

Unrecrystallized flat-rolled products exhibit a strong Brass $[\{110\}\langle 112\rangle]$ texture. The S $[\{123\}\langle 634\rangle]$ and copper $[\{112\}\langle 111\rangle]$ texture components are also present, but their intensities are not as high as those of the Brass texture component.

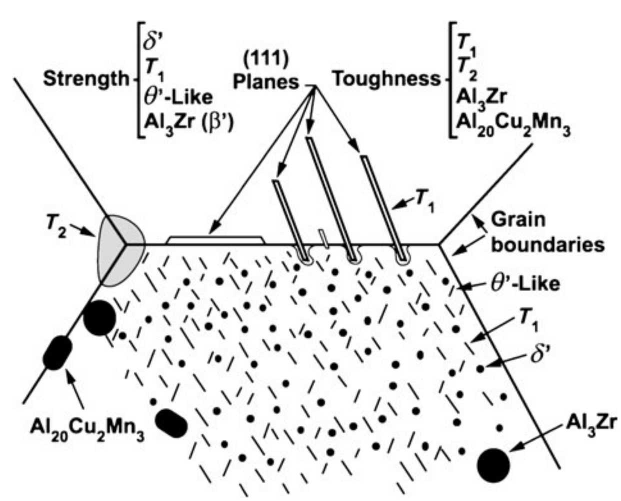

Fig. 1—Schematic precipitate microstructure in Al-Li 2099 and 2199 alloys.

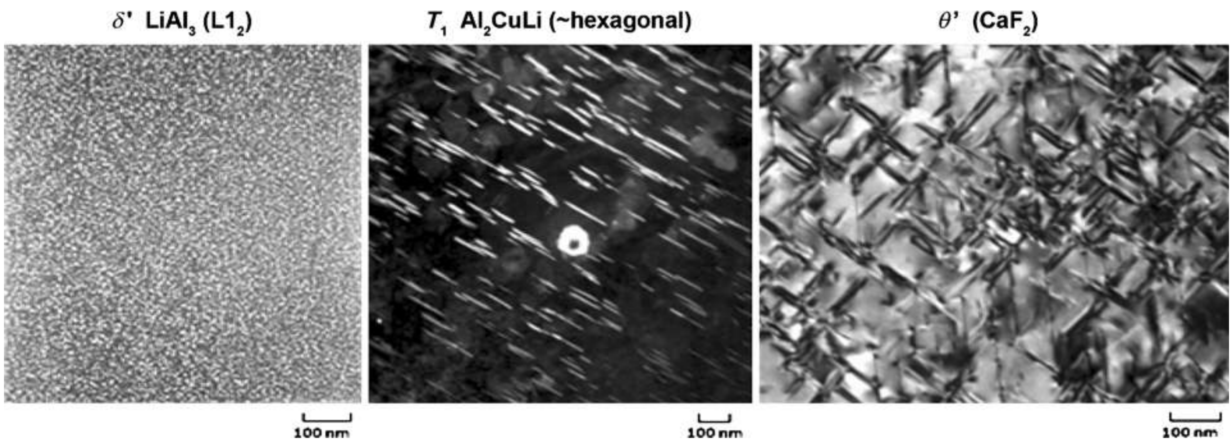

Fig. 2—Strengthening precipitates in 3rd-generation Al-Li alloys.

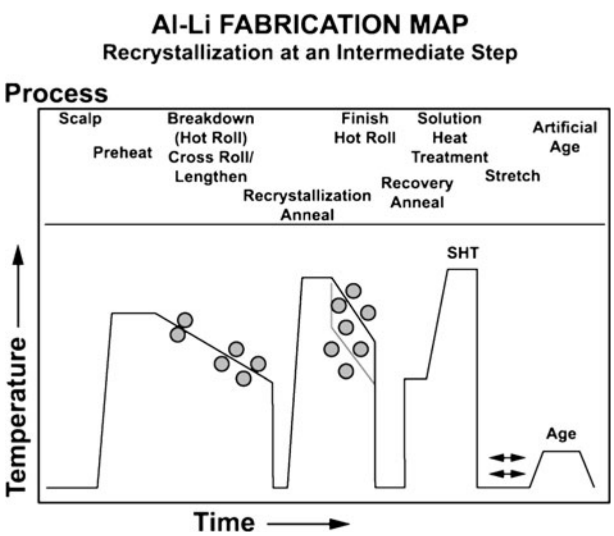

Fig. 3—Generic fabrication map for Al-Li plate products.

Recrystallized, flat-rolled products can exhibit strong Cube {001}⟨100⟩ and Goss {011}⟨100⟩ texture components. Typically, the Goss component is higher than Cube in a recrystallized sheet.[19]

A generic fabrication map for the unrecrystallized Al-Li plate products with low intensity of the "Brass" texture component is shown in Figure 3.

Al-Li alloys tend to form strong textures and texture gradients during fabrication, which lead to the anisotropy of mechanical properties, which can raise concern for designing and manufacturing (*e.g.*, forming and hole-expansion) as well as end use.[20–24] The recrystallization anneal is needed so recrystallization can occur at an intermediate gauge and not during solution heat treatment. This yields a final unrecrystallized microstructure with a moderate level of hot-deformation texture.

The optical micrographs of grain structures for Al-Li 2x99 extrusion, plate, and sheet are shown in Figure 4. For optimum mechanical properties, the extrusions and plate products are typically controlled to be unrecrystallized, whereas sheet products are typically recrystallized with elongated grains.

The texture of extruded products can be controlled with the use of "feeder plates" to yield different levels of anisotropy in mechanical properties.[25,26]

IV. SHORTCOMINGS OF "OLD" AL-LI PRODUCTS AND THEIR SOLUTIONS

Each of the following shortcomings of "old" Al-Li alloy products and its solutions will be discussed:

(a) High anisotropy of mechanical properties
(b) Crack deviation
(c) Low fracture toughness
(d) Microcracking during manufacture
(e) Poor corrosion resistance
(f) Loss of toughness after simulated thermal exposure (poor thermal stability)

Note that the examples used subsequently serve to demonstrate general solutions at the root cause. Specific composition, TMP, and flow paths used in 3rd-generation Al-Li products may vary from product to product.

A. *High Anisotropy of Mechanical Properties*

1. *The shortcomings*

- Second-generation Al-Li alloys (2090, 8090, and 2091) as unrecrystallized plate or sheet exhibit significantly lower strengths at 45 deg than the strength in the rolling direction. This is caused by strong crystallographic texture.
- Also, there is a high variability in the strength through the thickness.
- In-plane and through-thickness anisotropy lead to undesirable manufacturing characteristics.
- Because design is typically done with properties in the lowest direction, anisotropy in plane and through thickness makes 2nd-generation Al-Li products less competitive.
- Anisotropy must be minimized for ease of design, manufacture, forming, and end use.

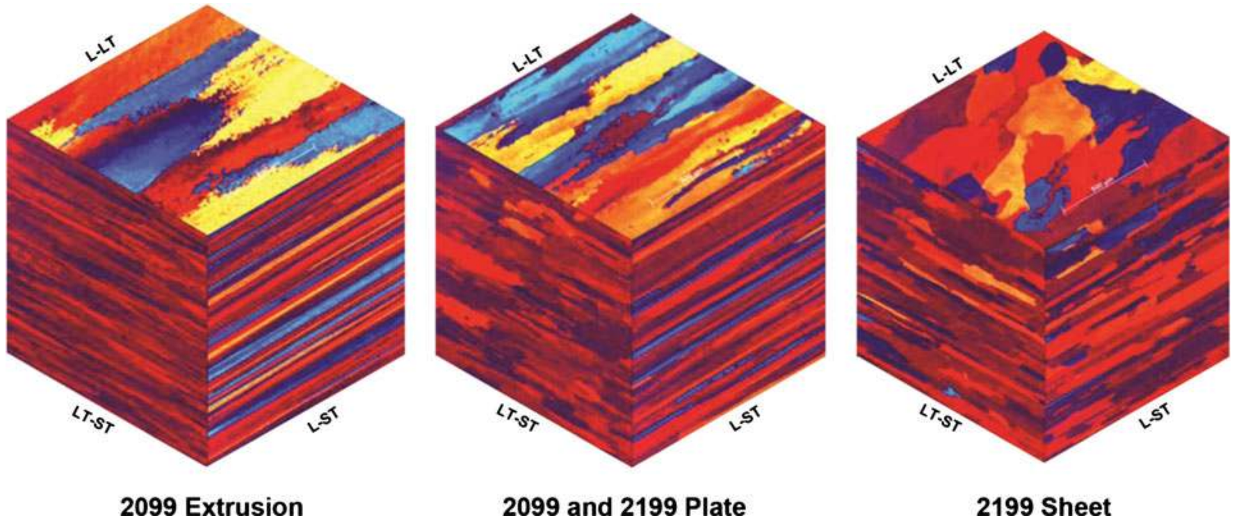

Fig. 4—Optical micrographs showing an extruded product with thin, elongated unrecrystallized grains; a plate product with elongated unrecrystallized grains; and a sheet product with recrystallized grains.

2. *Demonstration of solutions*

In-plane and through-thickness mechanical property anisotropy have their origin in the interactions among crystallographic texture, grain size, shape, cold deformation, and the precipitates developed during aging.[12,19–24,27–29] With the understanding of the root cause of anisotropy, solutions have been developed that combine composition optimization and innovative TMP. An example of a successful solution is demonstrated by alloy 2199 (C47A). Figure 5(a) shows the typically high in-plane strength anisotropy for a 2nd-generation Al-Li 8090 plate, which manifests in low strength at 45 deg from the rolling direction. Figure 5(b) shows the through-thickness strength anisotropy for the same 8090-T86 plate and 2199-T8E80 3rd-generation plate. Note that the 2199 plate shows similar strengths at thickness/2, thickness/4, and near surface in both the longitudinal (L) and long transverse (LT) orientations. Viz., unrecrystallized 3rd-generation 2199 plate shows minimal through-thickness and in-plane anisotropy.[19,30]

B. *Crack Deviation*

1. *The shortcomings*

High crystallographic texture (either high ''Brass'' in unrecrystallized or high ''Goss'' in recrystallized products) in conjunction with slip planarity yields to ''crack deviation'' during fatigue crack growth da/dN testing. Here, propagating cracks deviate from the expected direction of crack propagation, which makes it difficult to define locations for inspection or for the placement of crack arresters. In addition, it poses difficulties in structural design. A consortium was formed to address this issue consisting of: Deutsche Airbus, Alcan, Hoogovens, Defense Research Agency from U.K., and Alcoa.[29]

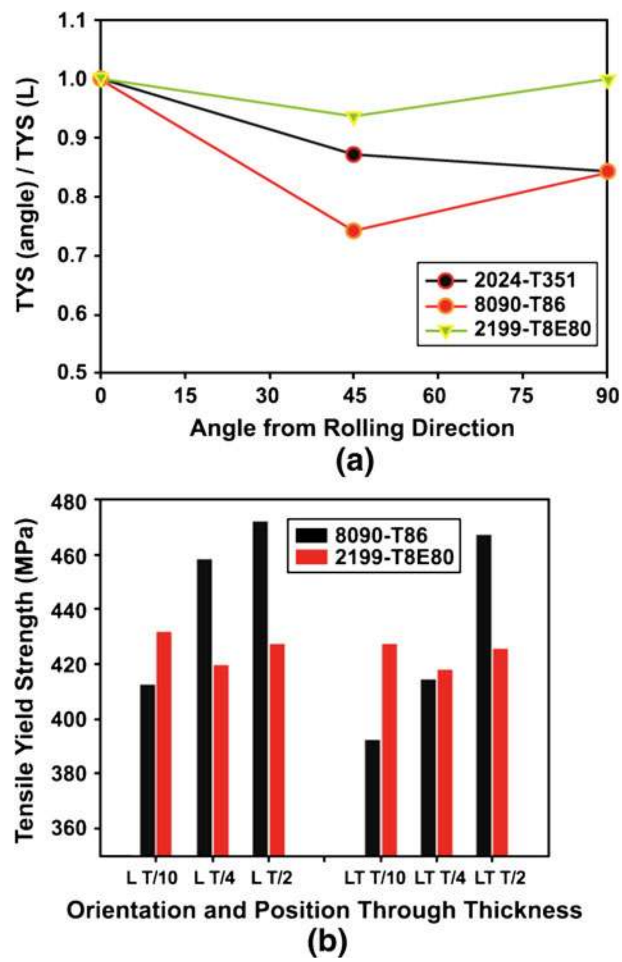

Fig. 5—(*a*) In-plane anisotropy of tensile yield strength for 3rd-generation 2199 and 2nd-generation 8090 plate. (*b*) Through-thickness anisotropy of tensile yield strength for 3rd-generation 2199 and 2nd-generation 8090 plate.

2. *Demonstration of solutions*

An example of the fatigue crack growth test specimen of 2nd-generation 8090 is shown in Figure 6.[29]

It was found that the reduction of the texture components was a necessary but not sufficient condition. In addition, the severity of slip planarity had to be decreased. This reduction was accomplished best by decreasing the amount of the δ' phase.[29] Control of the amount of δ' to a desired amount can be done in most instances by keeping the amount of Li additions at or below approximately 1.8 wt pct.[29] It was found that the grain size and shape had an effect also but were of secondary importance.

Successful mitigation of mechanical property anisotropy by composition optimization and control of crystallographic texture, grain size and shape, cold deformation, and amount and type of precipitates solved the crack deviation problem as reflected in the crack path of 3rd-generation Al-Li 2199 (C47A) (Figure 7). The crack is straight and perpendicular to the stress axis, unlike the 2nd-generation 8090-T86, which exhibited highly tortuous crack paths and crack deviation.

C. *Low Fracture Toughness*

Alloy 2024 and its variants have been the baseline material of choice for damage tolerance applications since the 1930s. Its success is reflected in the proliferation of its applications on most of today's aircraft. Consideration of new damage tolerant materials therefore requires a comparison with 2 × 24 alloys as a baseline. The fracture toughness of 2nd-generation 8090-T86 was often lower than incumbent 2024 alloy products for damage tolerance applications. 2 × 24 products have invariably used a T3 temper when high damage tolerance is needed. The microstructures in T3 tempers are typically free of precipitates at grain boundaries. In addition, a 2 × 24-T3 product only contains small clusters of solute as strengthening precipitates.[31] The fracture toughness, therefore, is affected only by insoluble second-phase particles.[32] The sought-after microstructures for high fracture toughness therefore contain the following:

- Precipitate-free grain boundaries
- Lowest possible amount of insoluble constituent second-phase particles
- Clusters or strengthening precipitates as small as possible
- Unrecrystallized or high aspect ratio recrystallized grains to maximize transgranular fracture

By composition optimization, TMP, and precipitate microstructure control, a 3rd-generation Al-Li alloy 2199 exhibits outstanding fracture toughness, as shown by the R-curves in Figure 8(a).

Short, transverse fracture toughness was also improved as the microstructure complied with the above principles. Figure 8(b) shows the short transverse specific strength and fracture toughness for a variety of "thick" plate products. Note the values measured for a 2nd-generation 8090-T87 plate. These are lower than the minima properties of the incumbent 7050-T7451 plate. The 3rd-generation plate products such as 2397, 2050, 2060, and Al-Li TP-1 exhibit improved strength/toughness relationships. In parentheses in Figure 8(b), note the density for these products (in gm/cm^3). Therefore, the shortcoming of low short transverse fracture toughness in 2nd-generation products was also overcome.

D. *Microcracking During Manufacture*

1. *The shortcomings*

A schematic representation of interference fit fastening process is shown in Figure 9. During insertion of interference fit fasteners, at high levels of interference, microcracks develop in the short transverse direction of 2nd-generation Al-Li alloys, which is not acceptable to original equipment manufacturers.[33]

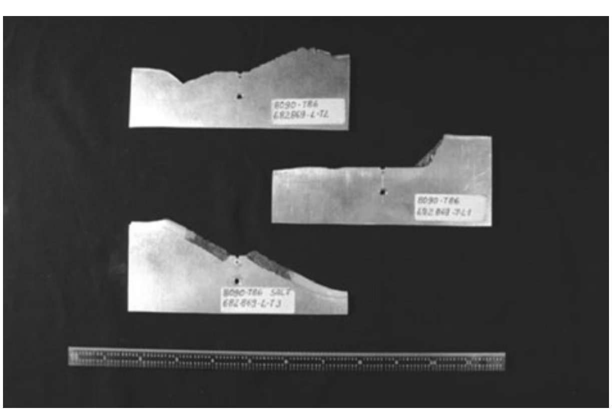

Fig. 6—Fatigue crack growth test specimen of 2nd-generation 8090 showing crack deviation. The stress axis is normal to the ruler.

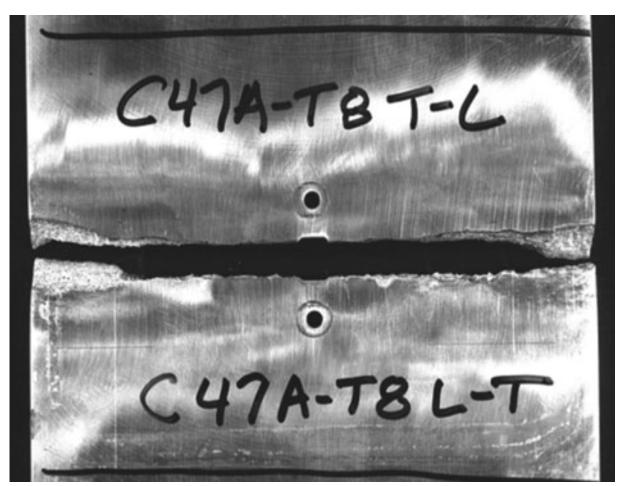

Fig. 7—Fatigue crack growth test specimen of 3rd-generation 2199 (C47A) showing straight crack path perpendicular to the stress axis. (Courtesy of Gary Bray).

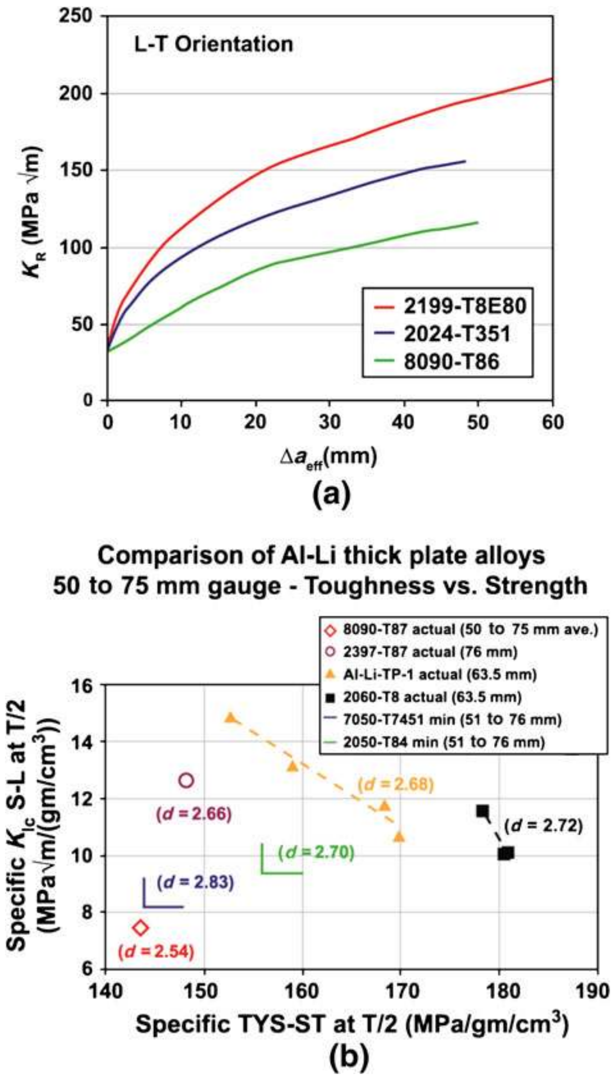

Fig. 8—(*a*) Plane stress fracture toughness R-curves for baseline 2024-T351, 2nd-generation Al-Li 8090-T86 with poorer toughness, and 3rd-generation Al-Li 2199-T8E80 with superior toughness. (Courtesy of Lynne Karabin). (*b*) Short transverse strength/toughness relationship for ''thick'' plate products (50 to 75 mm gauge). Note that 3rd-generation products exhibit improved performance over 2nd-generation 8090-T87 plate. (Courtesy of Julien Boselli).

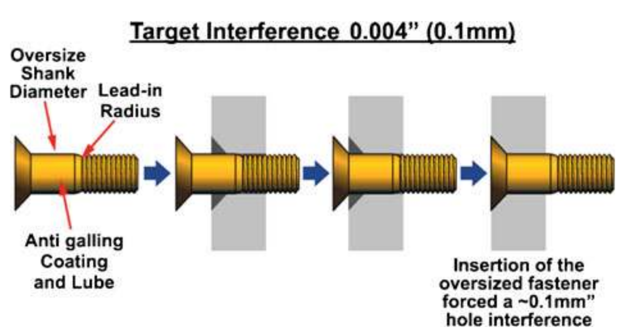

Fig. 9—Schematic of interference fit fastening process.

Typical levels of interference used in the aerospace industry are 0.006''. It has been reported that the 7075-T6 sheet can withstand levels above this level of interference without cracking; however, a 2090-T83 sheet required a reduced level of interference of 0.004'' to avoid the formation of cracks.[33]

2. *Demonstration of solutions*

It has been proposed that the excellent fatigue performance of Al-Li alloys may not necessitate interference fit fasteners for the required level of performance. Depending on the alloy and temper, the amount of work hardening and plastic deformation before cracking varies. Therefore it was proposed that the amount of interference should be tailored to each Al-Li product via experimentation.[33]

The root cause for cracking was found to be low elongation and work hardening ability in 2nd-generation products. Temper development for the 3rd-generation Al-Li products considered the use of lower amounts of cold deformation/stretch prior to aging and aging to tempers with a larger separation between tensile yield strength and ultimate tensile strength. This yielded higher elongation before fracture and higher work hardening.

As a result, testing done on 2099 and 2199 plate at 0.004'' interference and 2099 extrusions at 0.006'' interference have yielded crack-free fastened products. These evaluations are done by removing the fasteners after insertion and examining the holes in an SEM.

For example, using 2199-T8E80 plate the following experiment was conducted:

3. *Experimental details*

- 0.25-in (6.35 mm) diameter steel aerospace fasteners (NAS 1580)
- Interference fit of 0.004 in (0.1 mm)
- Two thicknesses of material: 0.25 in (6.35 mm) and 0.50 in (12.7 mm)
- Holes: two lubed and three nonlubed
- Examined metallographically and with SEM

4. *Results*

- No evidence of cracking with or without lubricant.

The results showed that by decreasing the level of interference and developing tempers with improved work-hardening characteristics, robust products can be made to avoid cracking during interference fit fastening.

Note that to date, several million pounds of 2099 extruded products have been used for the manufacture of fastened aircraft structures with no evidence of cracking using interference fit fasteners.

E. *Poor Corrosion Resistance*

1. *The shortcomings*

The 2nd-generation Al-Li products from alloys 2091 and 8090 as recrystallized sheet exhibited long transverse (LT) stress corrosion cracking (SCC) thresholds lower than those from the incumbents. In addition, the short transverse (ST) SCC resistance of unrecrystallized 8090 and 2090 plate products was also lower than that of their incumbents.

2. *Demonstration of solutions*

Table II shows that 3rd-generation Al-Li products provide significant improvements in exfoliation and SCC performance relative to non-Li incumbent products.

Tailoring both alloy composition and temper is critical in achieving a product with good corrosion performance and desirable structural characteristics such as damage tolerance. Several Al-Li alloys from Alcoa incorporate Zn additions for improved corrosion resistance.[30,34] In addition, aging studies demonstrate a "threshold" aging level, beyond which corrosion performance increases and remains unchanged. Examples of superior Al-Li products relative to incumbents with high strength, toughness, fatigue crack growth resistance, and corrosion resistance include 2099, 2199, 2096, C99N, and others.

Figure 10(a) shows only pitting with no exfoliation corrosion on 2099 products after close to 20 years of "sea coast" atmospheric exposure. More than 200 production lot release tests of 2099 were tested—they all exhibited MASTMAASIS corrosion ratings of P or EA. Figure 10(b) shows seacoast exposure results of 2099 at Point Judith, RI, for 19.1 years with no exfoliation and only pitting corrosion.

Figure 10(c) shows a schematic of the change in SCC resistance as a function of aging for 2099 plate in the ST direction. Note that a critical amount of aging is needed to achieve high SCC resistance. Also note that SCC

Table II. Stress-Corrosion Cracking Resistance of 2nd- and 3rd-Generation Products

Alloy-Temper	Orientation	SCC Threshold in Alternative Immersion (MPa/Ksi)	Generation
7050-T7451	ST	241/35	no lithium
2124-T851	ST	207/30	no lithium
8090-T86	ST	97/14	2nd generation
2090-T81	ST	172/25	2nd generation
2099-T86	ST	345/50	3rd generation
2199-T8E80	ST	>310/45	3rd generation
2096-T8X	ST	310/45	3rd generation

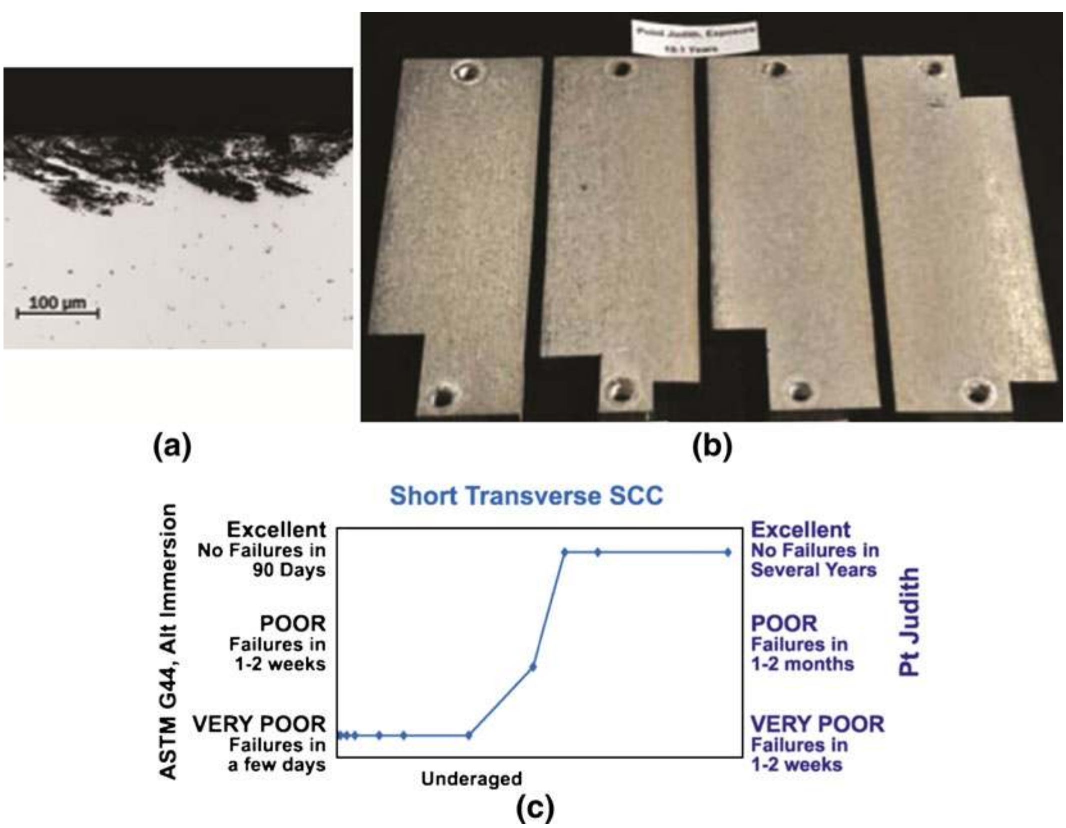

Fig. 10—(*a*) Pitting corrosion of 2099. (*b*) Seacoast exposure of 2099 at Point Judith for 19.1 years showing only pitting corrosion with a corrosion rating of P. (Courtesy of Jim Moran). (*c*) Schematic of SCC performance as a function of aging time. (Courtesy of Francine Bovard).

performance under alternative immersion correlates well with atmospheric exposure at the sea-coast site in Point Judith, RI.

The alloy 7050-T7451 developed by Alcoa has been used successfully for corrosion critical aerospace applications for about 40 years. Not only is 2099-T86 better in exfoliation rating than 7050-T7451, it is also better in Stress Corrosion Cracking resistance, as shown by numerous accelerated SCC tests and seacoast exposure data shown in Figure 11.

While the above examples are for Al-Li 2099 alloy, most 3rd-generation Al-Li products exhibit excellent corrosion resistance as reflected by many temper registrations and AMS specifications.

F. *Loss of Toughness After Simulated Thermal Exposure (Poor Thermal Stability)*

1. *The shortcomings*

Different structural components of an aircraft get thermal exposure to different thermal loads. These thermal loads can vary from deicing fluid in fixed leading edges in commercial aircraft to heating of bulkheads near the engine in fighter aircraft.

Although there is no universal test to simulate all types of thermal loads that a commercial aircraft may experience in wings and fuselage structures, exposures for 500 to 1000 hs in the range of 343 K to 358 K (70 °C to 85 °C) are often used to measure changes in performance. Fracture toughness was reduced significantly during simulated thermal exposure (1000 hs at 358 K [85 °C]) for 2nd-generation Al-Li products (2090, 8090, and 2190).[35–37] It was reported that even exposures to adhesive bonding degraded the toughness of 2091-T3 products.[36] In contrast, the slope of the strength/toughness relationship was shown to become less steep when a second step of aging was provided at temperatures lower than the first aging temperature, thereby reducing toughness loss.[37] An example of loss in fracture toughness for 8090-T86 plate after exposure of 1000 hs at 353 K (80 °C) is shown in Figure 12. References 38 and 39 show how multistep agings or ramped aging improve the thermal stability of Al-Li products.

2. *Demonstration of solutions*

Thermal stability needs to be considered during alloy design and temper development. From an alloy design perspective, it is required that the amount of alloying additions be sufficient to reach target properties at peak strength, viz., no solute should be left in solid solution that can come out as strengthening precipitates to change properties. From a tempering perspective, the aging to reach peak strength should be done with a final aging step as close as possible to the service temperature. This ensures that the supersaturation that develops, by the changing slope of the solvi, is released. Figure 13 shows the R-curves for 3rd-generation Al-Li alloy 2199-T8E80 with good thermal stability or no loss of toughness after thermal exposure. Both optimization of amount of solute and a multistep aging practice are required to attain a ''thermally stable'' product.

Another example of good thermal stability for an Al-Li fuselage sheet product (Al-Li 2060) is shown in Figure 14.

3. *Applying lessons learned to the 3rd generation of Al-Li alloys and products*

Chemical composition, TMP, and tempering were the main variables used to control the microstructural parameters and to overcome the shortcomings present in the 2nd generation of Al-Li products, viz., the products made from alloys 8090, 2090, and 2091.

Anisotropy of mechanical properties in plate and extruded products was reduced most significantly by controlling the crystallographic texture developed during TMP. In the case of sheet products, the control of recrystallization achieved this objective.

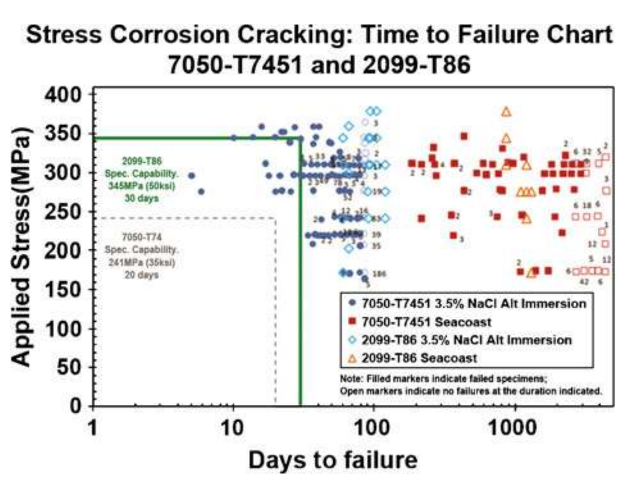

Fig. 11—Alternate immersion and seacoast stress corrosion test data showing superior stress corrosion cracking resistance of 2099-T86, even when compared with proven 7050-T7451. (Courtesy of Jim Moran).

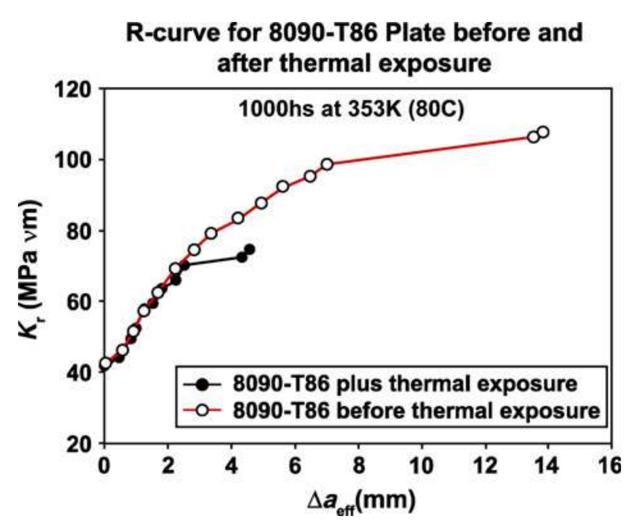

Fig. 12—R-curves for 2nd-generation Al-Li 8090-T86 plate showing loss of fracture toughness after thermal exposure. (Courtesy of John Newman).

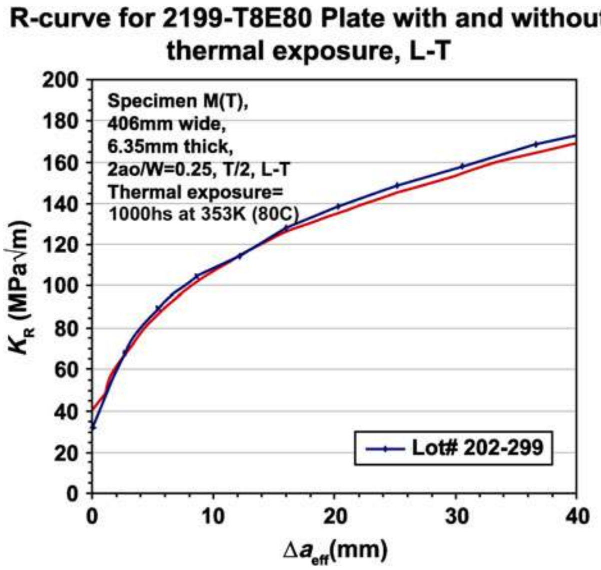

Fig. 13—R-curves for 2199-T8E80 plate before and after thermal exposure showing good thermal stability with no loss of toughness. (Courtesy of Lynne Karabin).

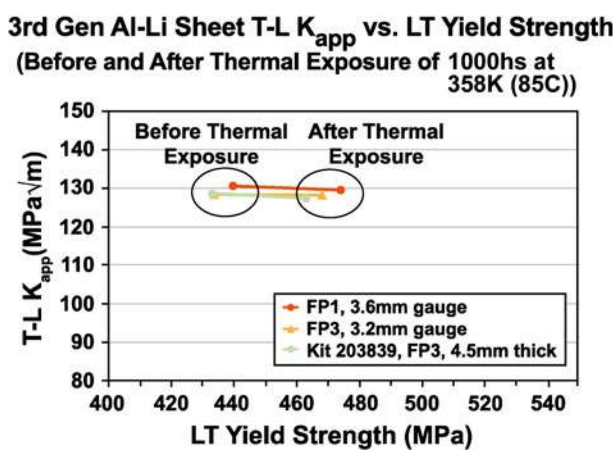

Fig. 14—T-L fracture toughness and LT yield strength cross plot showing 3rd-generation 2060-T8X sheet is thermally stable. (Courtesy of Paul Magnusen).

Control of the crack deviation required, in addition to texture control, a decrease in the severity of the planar slip. This was achieved primarily by limiting the amount of Li to control the amount of the δ' phase.

Low fracture toughness was addressed primarily by discouraging precipitation at the grain boundaries. This was accomplished in several ways, as follows:

(a) By decreasing the amount of solute, primarily the concentration of Li below 2 wt pct. This lowered the driving force for heterogeneous nucleation at grain boundaries.
(b) By increasing the amount of T_1/Ω precipitates.
(c) By reducing the amount of the δ' phase.
(d) By avoiding precipitation during the quench. This has limited availability of "heavy" gauge products for several alloys.

Microcracking during manufacture was addressed primarily by limiting the amount of interference during insertion of fasteners to 0.004". In addition, the plastic regime was increased by decreasing the amount of solute and decreasing the amount of cold deformation prior to aging.

The corrosion performance was improved mainly via alloying and tempering. Aging practices outside of the SCC susceptible regimes were used and alloying additions that yield improved corrosion resistance (such as Zn additions) were optimized.

The loss of toughness after simulated thermal exposure was addressed by discouraging precipitation at exposure temperatures. This was accomplished via the following processes:

(a) Reducing the amount of solute
(b) Aging closer to peak strength
(c) Providing multistep aging practices with the last step close to the exposure temperature to relieve supersaturation

Note that some of the alloy design changes affected several shortcomings of the 2nd-generation products at the same time, *e.g.*, a decrease in total amount of solute. As a result, the 3rd-generation products do not exhibit many of the shortcomings from the previous generation and have attained wider acceptance for aerospace and space applications.

V. REDUCED INSPECTION AND MAINTENANCE BURDEN

An added benefit for aerospace applications is that 3rd-generation Al-Li alloys exhibit improved spectrum fatigue crack growth (FCG) resistance.[19] This provides opportunities for increased inspection intervals and reduced maintenance burden, as shown by the lower wing panel test data in Figure 15.

Improvements in FCG are thought to be caused by both intrinsic and extrinsic factors. Most notably is the enhancement from crack closure effects caused by the tortuous crack path, which is characteristic of Al-Li base alloys.

VI. AL-LI PRODUCTS IN THE CONTEXT OF HISTORIC AEROSPACE PRODUCT EVOLUTION

To compare the improvements throughout the years in the performance parameters that size a given aerospace application, it is possible to examine three major parts of an aircraft structure viz., the upper wing, the lower wing, and the fuselage. For these, the following are the main sizing properties:

- Upper wing: Compressive yield strength and Modulus
- Lower wing: Fracture toughness (Plane stress K_{app}), ultimate tensile strength, and spectrum fatigue crack growth
- Fuselage: Fracture toughness (plane stress R-curve) and fatigue crack growth

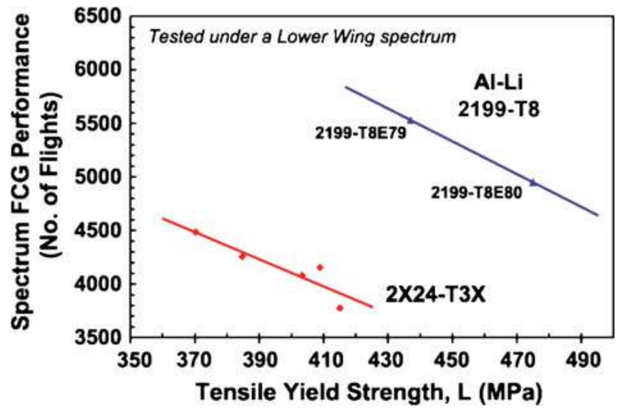

Fig. 15—Large aircraft lower wing spectrum fatigue crack growth curves comparing non-Li and 3rd-generation 2199 Al-Li lower wing plate in two different tempers.

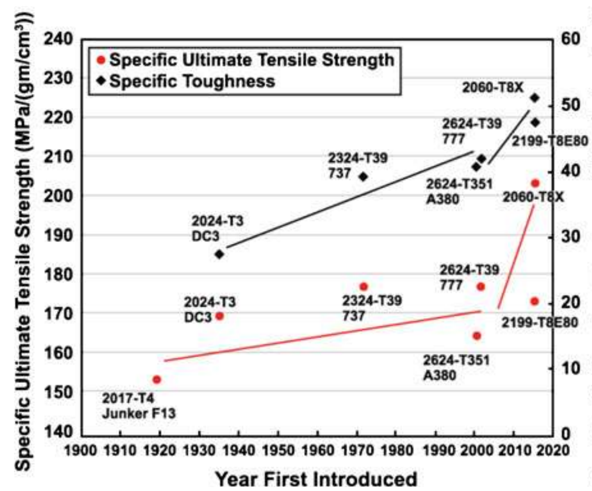

Fig. 17—Evolution of key properties for lower wings. (Courtesy of Lynne Karabin).

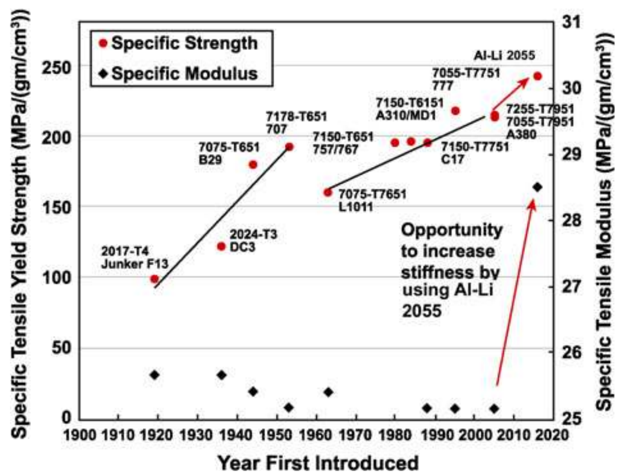

Fig. 16—Evolution of key properties for upper wings. (Courtesy of Diana Denzer).

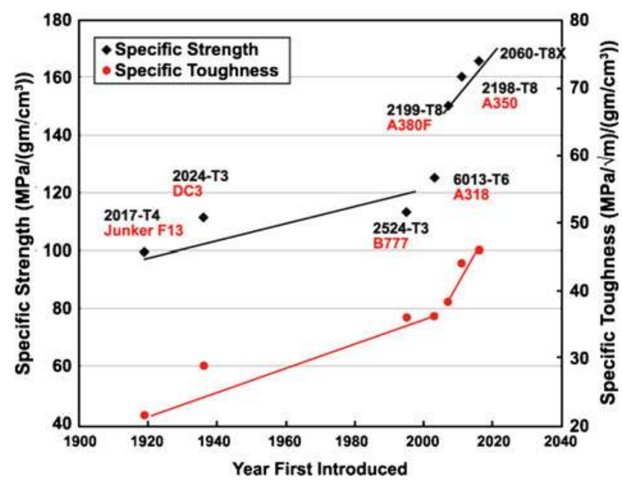

Fig. 18—Evolution of key properties for fuselage. (Courtesy of Paul Magnusen).

For rockets, the main sizing property is specific strength provided that the fracture toughness (KI_c) is high enough to prevent leakage.

Figures 16 through 19 show the improvements in the key properties for different major structural components of aircraft and spacecraft.

For upper wings, the specific compressive strength and the specific modulus tend to size the structure provided that fracture toughness is high enough. In Figure 16, the specific tensile yield strength is plotted (as a proxy for the compressive strength) *vs* the year of introduction for several aircrafts. Note the continuous increase of specific strength. During the 1930s to 1950s, the strategy was to increase the strength of the upper wing to decrease weight. However, corrosion issues, surfaced in the 707 aircraft, forced the compromise of strength and corrosion performance. This led to the replacement of T6 tempers with T7 tempers, such as T76, T77, and T79. These T7-type tempers exhibit improved exfoliation and SCC performance, but the modulus has remained constant for 7xxx products. This limits additional weight savings from buckling. Al-Li alloys, on the other hand, show a significant improvement in the modulus (as shown in Figure 16). This enables additional weight savings. The SCC and general corrosion of 3rd-generation Al-Li products is good as discussed previously.

In the case of lower wings, the specific ultimate tensile strength and the K_{app} fracture toughness size the application initially. Note in Figure 17, the continuous evolution in strength and fracture toughness and a significant increase in properties with 3rd-generation Al-Li products. Figure 17 shows two Al-Li alloys, *i.e.*, 2199 and 2060. The 2199 alloy contains more than twice the amount of Li present in 2060 as shown in Table I, which translates into slower fatigue crack growth for the alloy with the highest Li concentration. Therefore, depending on the mission of the aircraft and design criteria, it is possible to choose among 3rd-generation Al-Li products to optimize performance.

For fuselage applications, the key properties are the strength and fracture toughness in the LT direction (perpendicular to the rolling direction); this direction has the largest hoop stresses. Figure 18 shows the evolution of these properties for several major aircraft programs.

Note that the fuselage from 2060 sheet shows an improvement in both the strength and toughness.

Figure 18 shows three Al-Li sheet products (2199, 2198, and 2060 in T8 tempers). Note that with each new product, the specific strength and toughness continue to increase at a higher slope than with the non-Li incumbents.

For cryotankage used in the manufacture of rockets (akin to a pressure vessel), the specific strength translates into thinner membranes. The typical large rocket construction uses plate products machined with orthogrid or isogrid patterns to provide stiffness. Domes or gores for the ends of the fuel pressure vessels can be forged, stretch or spin formed, and welded via fusion or friction-stir welding methods. Large roll/forged aluminum rings are also used to connect the different fuel tanks and stages of a launch/space vehicle. Payload adaptors are used to connect the structure housing the payload to the rest of the launch vehicle in the case of most rockets. The space shuttle is different because it sits on top of the fuel tanks. Here, the payload/shuttle is attached to the main structure via an intertank structure. This structure enables the connection of the liquid fuel tanks and the space shuttle, which carries the payload.

The fuel tanks are pressure vessels that, in addition to high strength and stiffness, require adequate fracture toughness to prevent leakage. In the case of a pressure vessel, leakage is failure, and therefore, the relevant fracture toughness indicator is KI_e. Figure 19 shows the evolution in specific strength for a variety of aluminum products used since the onset of the space age (viz., the launch of Sputnik I). Note the significant jump in specific strength because of the use of Al-Li 2090 sheet and 2195 plate in the external tank of the space shuttle. Here, the 2090 sheet is used in the intertank structure, whereas the 2195 plate is used for the liquid hydrogen and liquid oxygen fuel tanks.

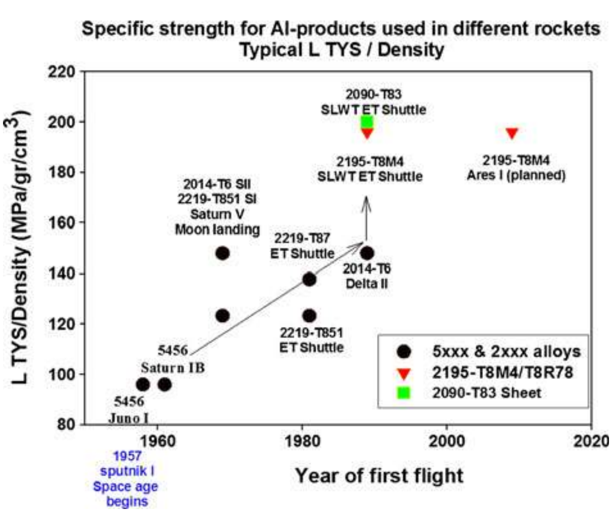

Fig. 19—Evolution of specific strength for products used in the manufacture of rockets.

VII. COROLLARY

- Al-Li alloy products have been in use for more than 50 years.
- Second-generation Al-Li alloys in the 1980s exhibited certain undesirable performance and manufacturing characteristics.
- Intense R&D since the early 1990s has resulted in the understanding of the underlying alloying and microstructural causes of the undesirable characteristics
- Third-generation Al-Li alloys have been developed by optimizing alloy composition, TMP, and tempering for a good balance of the following:
  - Density
  - Strength and toughness balance with low anisotropy of mechanical properties
  - Fatigue crack growth resistance
  - Corrosion resistance
  - Thermal stability
  - Manufacturability
- Third-generation Al-Li alloys have shown good progress toward successful major applications.
- R&D is continuing to commercialize 3rd-generation Al-Li alloy products tailored for all major structural application targeted at the following:
  - Weight savings
  - Performance enhancement
  - Reduced inspection and maintenance burden
- Al-Li products are well positioned to enable improved performance of next generation air and space craft.

ACKNOWLEDGMENTS

The authors thank the numerous colleagues who provided insight or data for this publication throughout the years. Special mention is made to D. Denzer, F. Bovard, and Drs. G. Bray, P. Magnusen, L. Karabin, J. Moran, and J. Boselli.

REFERENCES

1. W.M. Griffith: *Adv. Mater. Process.*, 2003, vol. 161, pp. 21–24.
2. E.A. Starke Jr. and J.T. Staley: *Prog. Aerosp. Sci.*, 1996, vol. 32, pp. 131–72.
3. E.S. Balmuth and R. Schmidt*: Proc. from First International Al-Li Conference*, Stone Mountain, GA, May 19-21, 1980.
4. E.A. Starke Jr.: *ICAS Proceedings*, September 7-12, 1986, pp. 934–43.
5. C.J. Peel, B. Evans, and D.S. McDarmaid: *Metall. Mater.*, 1987, vol. 3 (8), pp. 449–455.
6. E.J. Lavernia and N.J. Grant: *J. Mater. Sci.*, 1987, vol. 22, p. 1521.
7. W.E. Quist and G.H. Narayanan: *Treatise on Materials Science and Technology*, Academic Press Inc., New York, NY, 1989, vol. 31, pp. 219–54.
8. C.J. Peel: *The Development of Al-Li Alloys: An Overview*, AGARD LS 174, 1992.
9. I.M. Le Baron: US Patent 2,381,219, 1945-08-07.

10. I.N. Fridiyander, A.G. Bratukhin, and V.G. Davydov: *Soviet Al-Li Alloys of Aerospace Applications*, M. Peters and P.-J. Winkler, eds., DGM Informationsgesellschaft mbH, Germany, 1992, pp. 35–42.
11. P. Meyer and B. Dubost: *Production of Al-Li Alloy with High Specific Properties, Aluminum Lithium Alloys III*, The Institute of Metals, London, U.K., 1986, pp. 37–46.
12. R.J. Rioja: *Mater. Sci. Eng. A*, 1998, vol. 257, pp. 100–07.
13. R.J. Rioja and E.A. Ludwiczak: *Identification of Metastable Phases in Al-Cu-Li Alloys (2090) Al-Li Alloys III*, The Institute of Metals, London, U.K., 1986, p. 471.
14. S.C. Huang and M.J. Starink: *Int. Mater. Rev.*, 2005, vol. 50 (4), pp. 193–215.
15. R. Yoshimura, T.J. Konno, E. Abe, and K. Hiraga: *Acta Mater.*, 2003, vol. 51, pp. 4251–66.
16. W.A. Cassada, G.J. Shiflet, and E.A. Starke Jr.: *Metall. Trans. A*, 1991, vol. 22A, pp. 287–97.
17. W.A. Cassada, G.J. Shiflet, and E.A. Starke Jr.: *Metall. Trans. A*, 1991, vol. 22A, pp. 299–306.
18. R.J. Rioja, P.E. Bretz, R.R. Sawtell, W.H. Hunt, and E.A. Ludwiczak: *Proc. Int. Conf. on Al Alloys*, Chameleon Press, London, U.K., 1986, vol. 3, pp. 1781–87.
19. R.J. Rioja, C. Giummarra, and S. Cheong: *Light Metals,* David H. DeYoung, ed., TMS, Warrendale, PA, 2008, pp. 1065–69.
20. M.J. Bull and D.J. Lloyd: *Proc. from the Al-Li III Conf.*, The Institute of Metals, London, U.K., 1985, pp. 402–10.
21. K.V. Jata, A.K. Hopkins, and R.J. Rioja: *Mater. Sci. Forum*, 1996, vols. 217–222, pp. 647–52.
22. A.K. Vasudevan, W.G. Fricke, R.C. Malcolm, R.J. Bucci, M.A. Przystupa, and F. Barlat: *Metall. Trans. A*, 1988, vol. 19A, pp. 731–32.
23. A.K. Hopkins and R.J. Rioja: *Isotropic Al-Li Wrought Products-Final Report*, WL, MLLM, USAF Wright-Patterson AFB, 1996.
24. A.K. Vasudevan, W.G. Fricke Jr., M.A. Przystupa, and S. Panchanadeeswaran: *Proc. from ICOTOM 8*, TMS, Warrendale, PA, 1988, pp. 1071–77.
25. D.K. Denzer, P.A. Hollinshead, J. Liu, K.P. Armanie, and R.J. Rioja: *Texture and Properties of 2090, 8090 and 7050 Extruded Products*, vol. 2, DGM, 1992, pp. 903–08.
26. K.P. Armanie, R.J. Rioja, D.K. Denzer, C.E. Brooks, W.D. Cocker, D.K. Gadbery, and R. Newell: US Patent 6,113,711. 2000-09-05.
27. O.S. Es-Said and E.W. Lee: *Conf. Proc., Light Weight Alloys for Aerospace Applications*, Feb 13-16, 1996, MMMS/AIME, pp. 57–64.
28. N.J. Kim and E.W. Lee: *Acta Metall.*, 1993, vol. 41 (3), pp. 941–48.
29. R.J. Rioja: *Development of 8090 Sheet for Fuselage Applications*, Alcoa Technical Center Internal Reports, Alcoa Center, PA, 1991–1992.
30. C. Giummarra, R.J. Rioja, G.H. Bray, P.E. Magnusen, and J.P. Moran: *Proc. of the 11th Int. Conf. on Aluminium Alloys*, vol. 1, Aachen, Germany, September 22–26, 2008, pp. 176–88.
31. G.H. Bray, M.V. Glazov, R.J. Rioja, D. Li, and R.P. Gangloff: *Int. J. Fatigue*, 2001, vol. 23, pp. S265–76.
32. JT Staley: *American Chem. Soc.*, 1990, vol. 2, pp. 47–49.
33. H. Babel and C. Parrish: *Proc. from Westec 2004*, Los Angeles, CA, March 22–25, 2004.
34. R.J. Rioja, A. Cho, E.L. Colvin, and A.K. Vasudevan: US Patent 5,137,686. 1992-08-11.
35. C.D. Buscemi and E.S.C. Chin: *Microstruct. Sci.*, 1987, vol. 16, pp. 221–30.
36. M.V. Hyatt and S.E. Axter: *Proc. from "RASELM 91" Int. Conf. on Recent Advances in Science and Engineering of Light Metals*, Japan, 1991.
37. R.J. Rioja and R.S. James: US Patent No. 5,076,859, 1991-12-31.
38. H.J. Price: US Patent 5,879,481 B1 1999-03-09.
39. A.J.P. Haszler and C.J. Keidel: "US Patent 6,551,424 B1, 2003-04-22.